

02,08

Impedance measurement at intermediate frequency for an SIS mixer in the 1.1–1.4 mm range

© Ya.O. Vodzyanovskiy^{1,2,3}, K.I. Rudakov^{1,2}, I.V. Tretyakov¹, L.V. Filippenko², V.P. Koshelets^{2,3}, S.A. Kuznetsov^{4,5}, M.Yu. Arkhipov¹, A.V. Khudchenko¹

¹stro Space Center of P.N. Lebedev Physical Institute of the Russian Academy of Sciences, Moscow, Russia

² Kotelnikov Institute of Radio Engineering and Electronics, Russian Academy of Sciences, Moscow, Russia

³ Moscow Institute of Physics and Technology (National Research University), Dolgoprudny, Moscow Region, Russia

⁴ Rzhanov Institute of Semiconductor Physics SB RAS, Novosibirsk Branch „TDIAM“, Novosibirsk, Russia

⁵ Novosibirsk State University, Novosibirsk, Russia

E-mail: ya.vodzyanovskiy@lebedev.ru, khudchenko@asc.rssi.ru

Received April 18, 2024

Revised April 18, 2024

Accepted May 8, 2024

The work carried out an experimental measurement and numerical calculation of the impedance along the IF path for a superconductor-insulator-superconductor tunnel junction in a two-way mixer in the range of 1.1–1.4 mm. It has been shown that the power reflectance can vary from -30 to -5 dB depending on the operating point. An experimental method for determining the impedance of an SIS mixer has been proposed and tested

Keywords: superconductor–insulator–superconductor tunnel junction, intermediate frequency, submillimeter SIS mixer.

DOI: 10.61011/PSS.2024.06.58692.1HH

1. Introduction

Radio astronomy plays a key role in the development of hypersensitive mixers for heterodyne receivers, which are used to process electromagnetic radiation in the range of millimeter and submillimeter wavelengths. Superconductor–insulator–superconductor (SIS) tunnel junctions [1] constitute the basis for mixers (Figure 1), which have record noise characteristics in this range, close to the quantum limit. Mixers with sideband separation, consisting of two separate mixing systems are the most common among ground receivers [2,3]. It is necessary to ensure a low level of reflections of SIS mixers for the receiver to work effectively. This is important as at the mixer input at the frequency of the received signal (HF) [4,5], and at the output at an intermediate frequency (IF, IF). A theoretical calculation of the impedance of the SIS mixer at the IF output was made in this paper, and an experimental measurement of the reflection level was performed for minimizing it in the future.

The objective of the experiment is to measure the level of reflection from the mixing system via the intermediate frequency output channel (IF), when an offset voltage is applied to the mixer and a high-frequency local oscillator (LO) signal is applied. The measurements were performed in the range of 2–12 GHz; this range is determined by the band of the cryogenic IF amplifier used. The scheme of the experiment is shown in Figure 2; the SIS mixer is placed in

closed cycle cryostat at temperature of about 4 K. The signal of the high-frequency local oscillator (LO) enters the mixing system through the beam separator and horn. The vector network analyzer (VNA), located outside the cryostat, generates a test signal of the range of 2–12 GHz on the port (P1), which, passing through the attenuator -10 dB, enters the directional coupler which directs it to a mixing system with a coupling coefficient of about -10 dB. Next, the signal passes through a bias tee, which allows the IF signal to pass

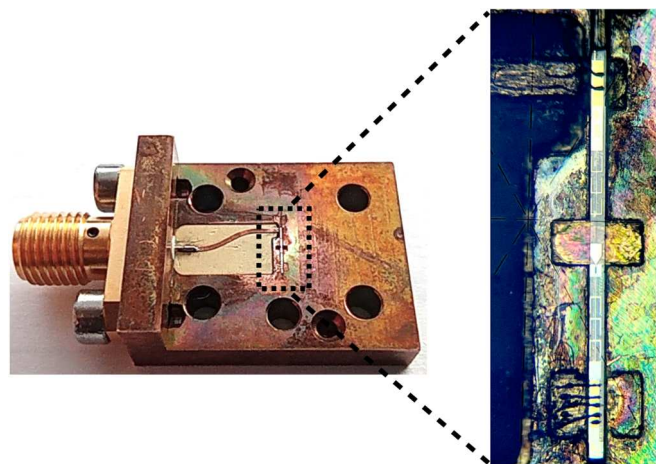


Figure 1. A photo of the Back piece with the mixer chip installed.

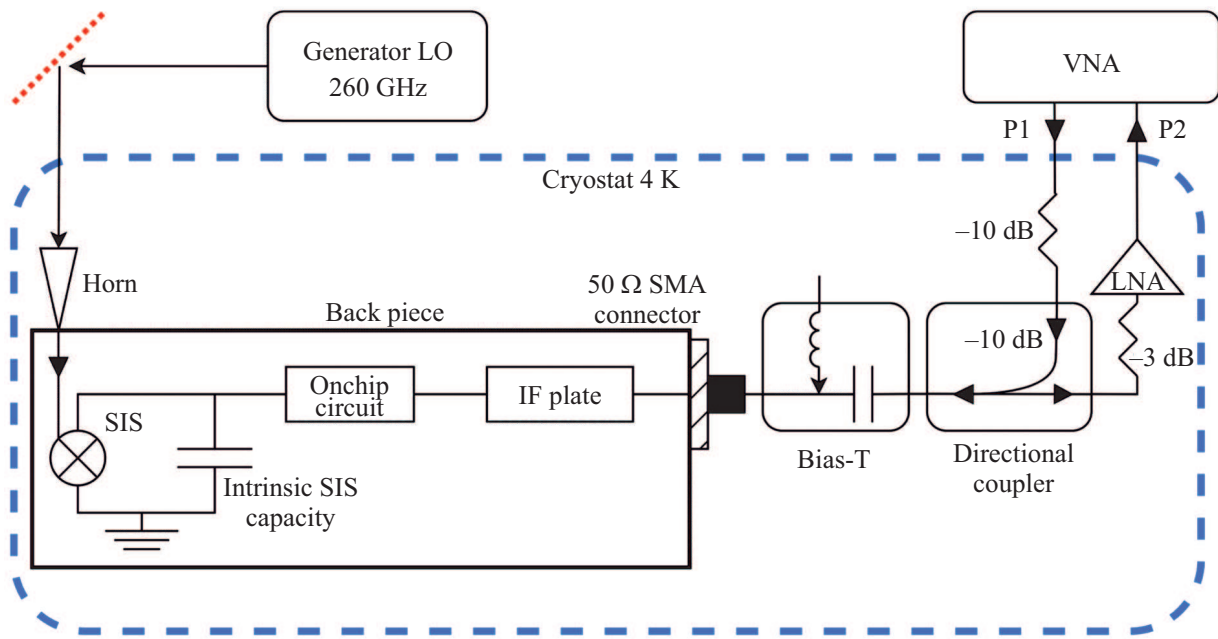


Figure 2. Scheme of the experiment on measuring the reflection from the SIS mixer for the IF output.

unhindered, while setting the voltage on the SIS mixer for direct current through a large inductance. After bouncing off the SIS mixer, the main part of the signal passes directly through the directional coupler and is fed to the input of a cryogenic low noise amplifier (LNA), which amplifies this signal and sends it to the receiving port (P2) of the VNA. In fact, the measured parameter is the ratio of the VNA signals on ports P1 and P2, or rather, its spectrum.

2. Calibration

An important step in the experiment is the calibration of the VNA in order to improve the accuracy of measurements. We use a standard single-port calibration, details are set out in [6], which is based on the definition of 3 circuit parameters: D — direct leakage in the circuit, R — internal reflections, M — misalignment

$$S_{11} = \frac{S_{11_m} - D}{R + M(S_{11_m} - D)}, \tag{1}$$

where S_{11} — the actual reflection coefficient, and S_{11_m} — the measured reflection coefficient.

In calibration measurements at 4 K the SIS junction itself is used as a calibrator [7]. Figure 3 illustrates which bias voltages are used for calibration. Bias voltages, differential resistances and reflection coefficients used for calibration are listed in the table.

3. Measurements

Current-voltage curve of the mixer with applied signal of the local oscillator with frequencies of 234, 255,

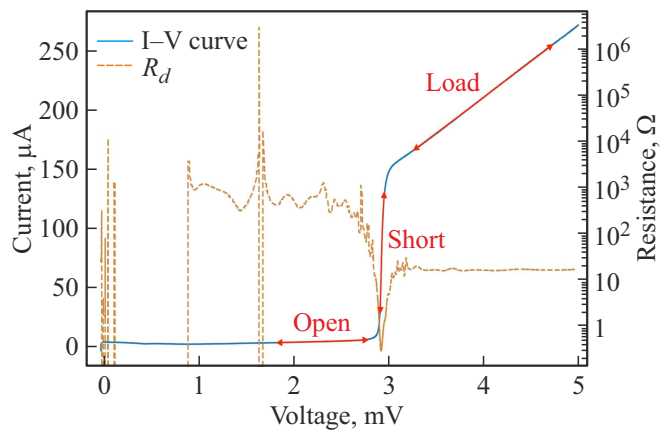


Figure 3. The autonomous current-voltage characteristic of the mixing system (I – V curve) is a blue solid line; the corresponding differential resistance (R_d) is shown by an orange dashed line.

262 GHz in „operating“ mode, shown in Figure 4. The „operating“ bias voltage is approximately in the range of 1.8–2.6 mV. This voltage region corresponds to the so-called quasiparticle step caused by the application of a local oscillator signal to the SIS junction. The power of the local oscillator was adjusted using the quasi-optical attenuator based on a subwavelength polarization array of 1-dimensional aluminum conductors (width/lateral period: $4/8 \text{ m}\mu$) photolithographically manufactured on the surface of a carrier polypropylene film with a thickness of $4 \text{ m}\mu$ [8].

The change in the level of reflections with varying bias voltage of the SIS mixer is shown in Figure 5. The results of reflection measurements at IF 2, 4, 6, 8, 12 GHz are

Bias voltages, differential resistances and reflection coefficients used for calibration

	Bias voltage, mV	Differential resistance, Ω	Reflection coefficient, dB
Open circuit	2	450	-1.94
Short circuit	2.912	0.33	-0.117
Loaded circuit	4	16	-5.81

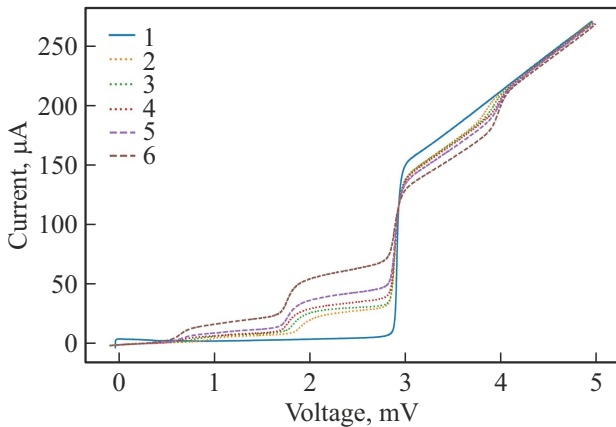


Figure 4. Current-voltage curve of the mixer: self-contained solid blue curve №1; when the LO signal is applied at frequencies of 234, 252, 266 GHz for the first pumping level, dotted curves №2, 3, 4, respectively; when the LO signal is applied at a frequency of 266 GHz at the second and third pumping levels, dashed lines №5, 6, respectively.

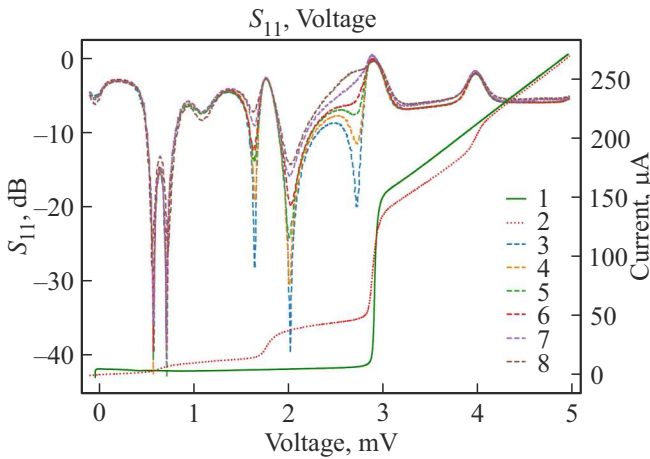


Figure 5. The current-voltage curve of the mixing system: autonomous №1 green curve loaded with the signal of the local oscillator 266 GHz №2 red dotted. Reflection measurement results dotted curves №3, 4, 5, 6, 7, 8 for the IF 2, 4, 6, 8, 10, 12 GHz, respectively.

shown here. It can be seen that the reflection level decreases significantly at a voltage of 2.7 mV. This absorption peak can be explained by the fact that the impedance of the mixing system becomes almost equal to the impedance of the IF

supply line based on the formula [9]:

$$S_{11_{IF}} = \frac{Z_{IF} - Z_L}{Z_{IF} + Z_L} \tag{2}$$

It is important to note that the minimum reflection level is determined by the modulus of the difference between the imaginary components of the impedances of the SIS mixer and the supply line. Additionally, it is possible to see the dependence of the absorption peak on the selected frequency, the higher the frequency, the higher the reflection level.

The dependence of the reflection level on frequency is shown in more detail in Figure 6, where the experimental frequency dependences S_{11} are given at different voltages on the SIS mixer. The above results demonstrate that the reflection level almost does not change with frequency at a bias voltage of 4.5 mV in the IF range of 2–12 GHz, however, we clearly see a frequency dependence for bias voltages of 2.1 and 2.4 mV.

Figure 7 shows the measured impedance of the SIS mixer from the voltage at different bias voltages and frequency segments. Dotted curves №4.1, 5.1, 6.1, 7.1, 8.1 -show the actual part of the impedance, and the dashed curves №4.2, 5.2, 6.2, 7.2, 8.2 show the imaginary part of the impedance for IF of 2–4, 4–6, 6–8, 8–10, 10–12 GHz.

Figure 8 shows the dependences of the actual and imaginary parts of the impedance on the intermediate

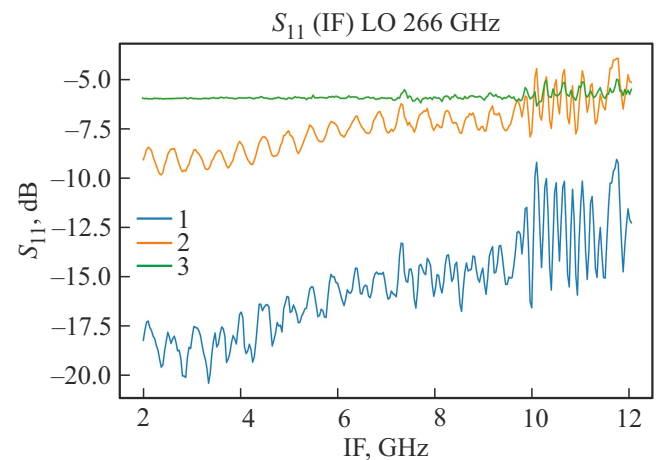


Figure 6. The experimentally determined level of reflection from the mixer system in the „operating mode“ with the applied LO signal of 266 GHz. The voltage of the SIS mixer №1–2.1 mV, №2–2.4 mV, №3–4.5 mV.

frequency in comparison with the differential resistance at bias voltages of 2.2, 2.5, 4.5 mV. It can be seen that the imaginary part of the impedance decreases with frequency, thereby increasing the level of reflection. However, we do not see a frequency dependence at a bias voltage of 4.5 mV and the imaginary part of the impedance is close to 0 Ω.

Figure 9 shows the dependence of the noise temperature on the IF, a noticeable increase of T_n can be noted after ~ 8 GHz which is directly related to the increase of the modulus of the imaginary part of the impedance of the SIS mixer and the reflection level.

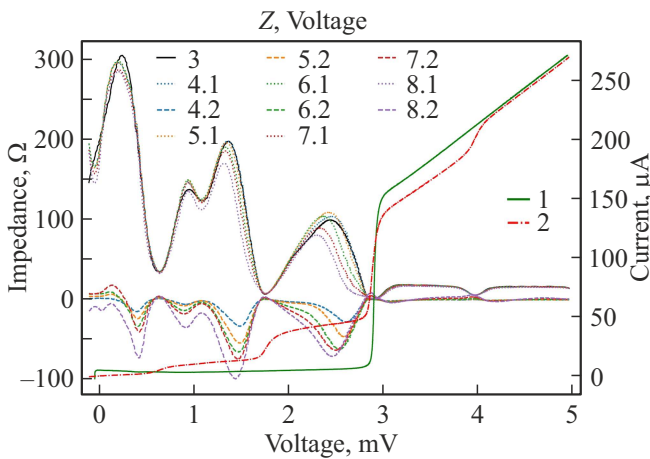


Figure 7. The current-voltage curve of SIS mixer is autonomous and in „operating mode“ with the applied LO signal of 266 GHz № 1 solid green and № 2 dashed red curves, respectively. Differential resistance № 3 black solid curve. Experimentally determined impedance of the mixing system in „operating mode“ at the frequency ranges of 2–4, 4–6, 6–8, 8–10, 10–12 GHz for curves № 4.x, 5.x, 6.x, 7.x, 8.x, respectively, where the dotted curves show the actual impedance, and the dashed curves show the imaginary parts of the impedance.

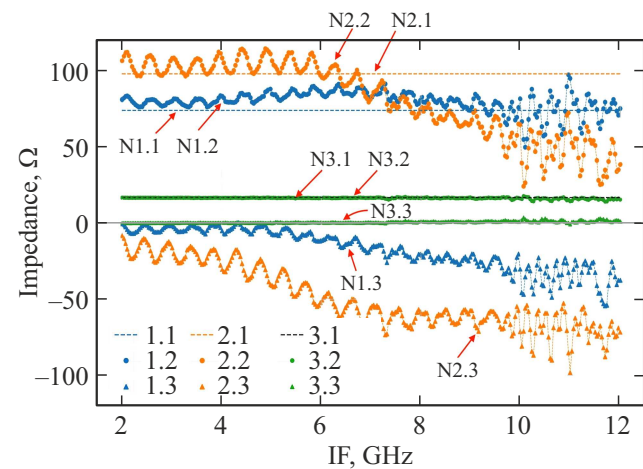


Figure 8. Frequency dependence of the impedance of the SIS mixer; curves № 1.x, 2.x, 3.x show bias voltages of 2.2, 2.4, 4.5 mV, respectively; curves № x.1 show differential resistance, curve № x.2 show the actual part of the impedance, curve № x.3 show the imaginary part of the impedance.

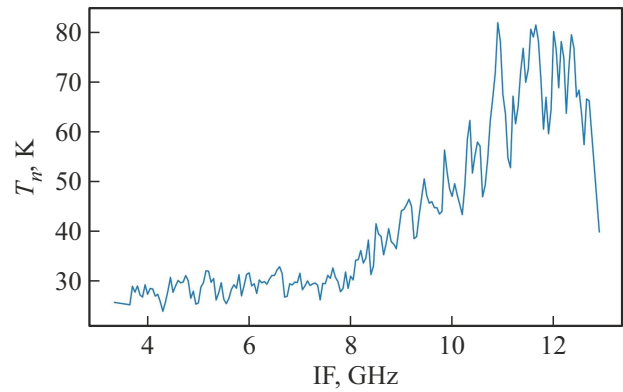


Figure 9. Dependence of the noise temperature on the IF with applied LO signal 267 GHz [10].

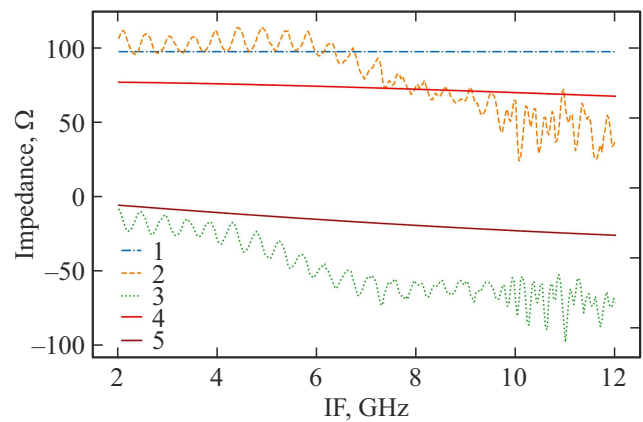


Figure 10. Frequency dependence of the impedance of the mixing system: № 1 — differential resistance, № 2 — actual experimental impedance, № 3 — imaginary experimental impedance, № 4 — actual theoretical impedance, № 5 — imaginary theoretical impedance.

The reflection from the SIS receiver is characterized by the parameter S_{11} , which is expressed in terms of the intrinsic impedance of the SIS junction Z_{IF} and the impedance of the supply line Z_L through the formula (2). The impedance of the SIS junction can be calculated using a three-frequency approximation to the theory of quantum displacement [1], the final formula has the following form

$$Z_{IF} = \|Y_{mm'} + Y_m \delta_{mm'}\|_{11}^{-1}, \quad (3)$$

where $Y_{mm'}$ — 3×3 conduction matrix linking the components of currents and voltages in the mixer, Y_m — high frequency impedance vector of the supply line, $\delta_{mm'}$ — the Kronecker symbol, Z_{IF} — the central element with the indices (1,1) of the calculated inverse matrix.

Figure 10 shows a comparison of differential resistance (blue dashed dotted curve № 1), experimental (orange dashed № 2 — real; green dotted № 3 — imaginary) and theoretical (red solid № 4 — actual; brown solid № 5 — imaginary) impedances of frequency.

Figure 11 shows a comparison of the experimental and theoretical impedances from the bias voltage. The experi-

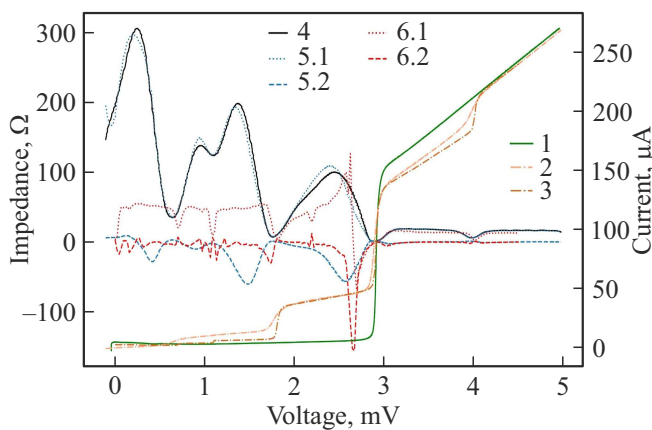


Figure 11. current-voltage curve of the SIS mixer: №1 green solid curve — autonomous, №2 pink dotted curve — working experimental, №3 dashed orange curve — working theoretical. The dependence of the impedance of the SIS mixer on the voltage: №4 solid black curve — differential resistance, №5.1 dotted blue curve — actual experimental impedance, №5.2 dashed blue curve — imaginary experimental impedance, №6.1 dotted red curve — actual theoretical impedance, №6.2 dashed red curve — imaginary theoretical impedance.

mental impedance is averaged in the window IF 5–7 GHz, the theoretical impedance is calculated for IF 6 GHz.

4. Conclusion

The paper proposes a method that combines experimental and theoretical determination of the parameters of the SIS junction, such as impedance and reflection level. This method allows studying the relationship between the level of reflections from the mixing system at the IF output and the bias voltage, as well as the power of the reference signal. The determination of the parameters of the SIS junction in combination with the modeling of the elements of the IF channel will allow in the future the calculation with high accuracy of the IF characteristics of the mixer itself, as well as the entire receiver created on its basis.

Funding

The work was supported by the Russian Science Foundation grant No. 23-79-00061 (<https://rscf.ru/project/23-79-00061/>). The technology of manufacturing tunnel junctions was trialed at the Kotelnikov Institute of Radio Engineering and Electronics of RAS as part of a state assignment. Unique Scientific Facility (USF) No. 352529 „Cryointegral“ was used for the preparation and study of samples. Its development was supported by a grant from the Ministry of Science and Higher Education of the Russian Federation, agreement No. 075-15-2021-667.

Conflict of interest

The authors declare that they have no conflict of interest.

References

- [1] J.R. Tucker, M.J. Feldman. *Rev. Mod. Phys.* **57**, 4, 1055 (1985). DOI: 10.1103/RevModPhys.57.1055
- [2] V. Belitsky, M. Bylund, V. Desmaris, A. Ermakov, S.E. Ferm, M. Fredrixon, S. Krause, I. Lapkin, D. Meledin, A. Pavolotsky, H. Rashid. *Astronomy Astrophys.* **611**, A98 (2018).
- [3] J.Y. Chenu, A. Navarrini, Y. Bortolotti, G. Butin, A.L. Fontana, S. Mahieu, D. Maier, F. Mattiocco, P. Serres, M. Berton, O. Garnier, Q. Moutote, M. Parioleau, B. Pissard, J. Reverdy. *IEEE Trans. THz Sci. Technol.* **6**, 2, 223 (2016).
- [4] R. Hesper, A. Khudchenko, A.M. Baryshev, J. Barkhof, F.P. Mena. *IEEE Trans. THz Sci. Technol.* **7**, 6, 686 (2017)
- [5] A. Khudchenko, R. Hesper, J. Barkhof, F.P. Mena, A.M. Baryshev. In: *IEEE 2019 44th Int. Conf. Infrared, Millimeter, Terahertz Waves (IRMMW-THz)* (2019). P. 1–2.
- [6] Y.O. Vodzyanovsky, A.V. Khudchenko, V.P. Koshelets. *FTT* **64**, 10, 1385 (2022)
- [7] P. Serres, A. Navarrini, Y. Bortolotti, O. Garnier. *IEEE Trans. THz Sci. Technol.* **5**, 1, 27 (2015).
- [8] A.A. Mamrashev, N.A. Nikolaev, S.A. Kuznetsov, A.V. Gelfand. *AIP Conf. Proc.* **2300**, 020083 (2020). DOI: 10.1063/5.0031931
- [9] J.W. Kooi. *Advanced Receivers for Submillimeter and Far Infrared Astronomy*. Print Partners Ipskamp B.V., Enschede, The Netherlands (2008). ISBN 978-90-367-3653-4.
- [10] K.I. Rudakov, P.N. Dmitriev, A.M. Baryshev, A.V. Khudchenko, R. Hesper, V.P. Koshelets. *Izv. vuzov. Radiofizika LXII. Vyp. 7–8*, 613 (2019). (in Russian).

Translated by A.Akhtyamov